

# Error Modelling and Sensitivity Analysis of a Planar 3-PRP Parallel Manipulator

Jayant K. Mohanta<sup>1</sup>, Santhakumar Mohan<sup>1(✉)</sup>, Mathias Huesing<sup>2</sup>,  
and Burkhard Corves<sup>2</sup>

<sup>1</sup> Mechanical Engineering, Indian Institute of Technology (IIT) Indore,  
Indore 453552, India

{phd1401103005, santhakumar}@iiti.ac.in

<sup>2</sup> Department of Mechanism Theory and Dynamics of Machines,  
RWTH Aachen University, Aachen 52072, Germany  
{huesing, corves}@igm.rwth-aachen.de

**Abstract.** This paper presents an analytical error prediction model of a 3PRP planar parallel manipulator using the screw theory. This analytical approach is used to find the effect of mechanical inaccuracies contributing to the end-effector pose errors and their sensitivity coefficients. Finally, parameter sensitivity analysis of non-compensable errors of two different configurations based on their fixed base shape namely  $\Delta$ -shape and U-shape fixed bases are analysed and compared.

**Keywords:** Planar parallel manipulator · Error modelling · Sensitivity analysis · Non-compensable errors · Mechanical inaccuracies

## 1 Introduction

Planar parallel manipulators (PPMs) are having higher attention in the recent years due to their simplicity in design and other potential advantages over serial manipulators [6]. In specific, manipulators having first joint as active prismatic joint in each leg has several advantages than others [5]. In this respect, one of the commercially available manipulators namely Hephaist [3] is a 3PRP U-shape PPM and the manipulator proposed by Damien Chablat *et al.* is a  $\Delta$ -shape 3-PRP PPM [1], both of them are promising in terms of their kinematic and dynamic performances. This 3PRP configuration has shown potential advantage in industrial usage but which of these two base configurations is better in terms of accuracy in presence of mechanical inaccuracies are yet to be explored. Accuracy analysis of these configurations due to the actuator inaccuracies using the geometric approach is presented by Yu *et al.* [8], but in this work, effect of other non-compensable errors and kinematic parameter errors are not included. It is significant to quantify the sources of errors which are contributing the end-effector pose errors in order to find the quality of task performed by the manipulator, which directly affects the positional accuracy of the manipulator. These pose errors can be of three kinds: kinematic errors, encoder errors and the errors due to joint clearances.

The kinematic errors are due to the misalignments and the manufacturing imperfections and tolerances. These kinematic errors for manipulators can be estimated and many researches has found methods to quantify and compensate them [3, 4]. Encoder errors can be of two types, the first one is due to least count of the encoders and other one is due to incorrect index of the encoder reading. Index errors can be corrected by zero point confirmation, but least count errors are non-compensable. Similarly, error due to joint clearances and backlashes are also non-compensable in nature.

Therefore, in this paper, a complete error prediction model considering all possible errors i.e., due to mechanical inaccuracies (including the kinematic parameter errors and error due to joint clearances in the rotary and prismatic joints which are non-compensable in nature) based on screw theory [2] is derived and presented. This technique is already been utilized and verified by G. Wu *et al.* [7] for modelling the error prediction model for 3-PPR configuration. This configuration has a simple model due to its forward kinematics relationship, which is independent of its end-effector orientation. But, in case of 3-PRP configuration, the kinematic relationship is dependent on the end effector orientation. The proposed mathematical error model has incorporated all these changes and used it for the error sensitivity analysis. This errors estimation is done for the  $xy$ -plane only, the error  $z$ -axis is not derived in this model as manipulator functioning is restricted to  $xy$ -plane only. Further, the effects of the non-compensable errors are compared to identify the best configuration among U-shape and  $\Delta$ -shape fixed base configurations (which one is less susceptible to the non-compensable errors).

## 2 Kinematic Model of the Manipulator

Here in this section, a generalized kinematic solution for the 3PRP configuration is presented. This kinematic model is established on the basis of screw theory. The kinematic arrangement of the 3PRP configuration is presented in Fig. 1. In Fig. 1, the point  $T$  is the position of the end-effector and  $\varphi$  is its orientation angle, the point  $O$  represents the origin of the frame of reference, points  $G_i$ ,  $P_i$ ,  $R_i$  and  $F_i$  represent the beginning limit of the linear actuators, the current position of the linear actuators, the point where the passive prismatic joint starts and the point at which the prismatic link connects to the end effector of the  $i^{th}$  link, respectively. The vectors  $\mathbf{i}_i$ ,  $\mathbf{j}_i$ ,  $\mathbf{k}_i$ ,  $\mathbf{l}_i$  and  $\mathbf{m}_i$  are the vectors leading from the fixed reference frame (origin) to the end-effector (moving reference frame). Representation of the each vector for the first kinematic chain (leg) is shown in Fig. 1, and it is similar to the other kinematic chains with corresponding index number. These vectors are characterized by the angles  $\alpha_i$ ,  $\beta_i$ ,  $\gamma_i$ ,  $\theta_i$ ,  $\varphi$  and  $\psi_i$ , where angles  $\alpha_i$ ,  $\beta_i$ ,  $\gamma_i$ ,  $\theta_i$  and  $\varphi$  are with respect to the origin reference frame while  $\psi_i$  is with respect to end-effector's reference frame and  $i = 1, 2, 3$ , which is the index of the kinematic link chain.

From the closed looped kinematic chain  $O - G_i - P_i - R_i - F_i - T - O$

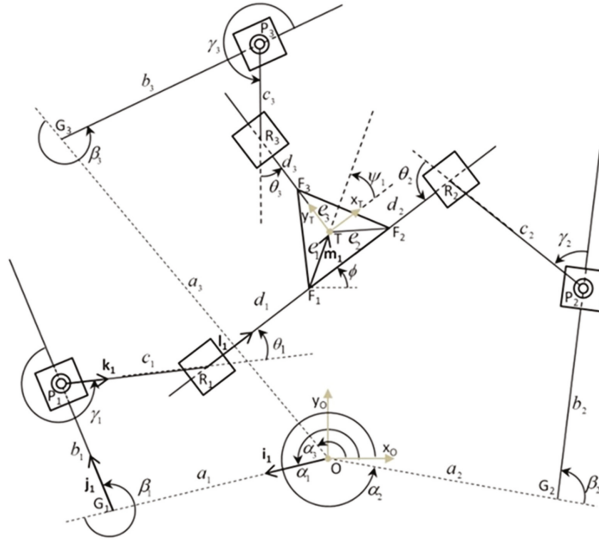


**Fig. 1.** Generalized kinematic parameter diagram for 3PRP manipulator

Forward kinematics equation for the position vector of the end-effector,  $\mathbf{T}$ , is given as:

$$\mathbf{T} = a_i \mathbf{i}_i + b_i \mathbf{j}_i + c_i \mathbf{k}_i + d_i \mathbf{l}_i + e_i \mathbf{m}_i, \quad i = 1, 2, 3 \quad (1)$$

$$\text{With, } \mathbf{i}_i = [\cos \alpha_i \sin \alpha_i]^T, \mathbf{j}_i = [\cos \beta'_i \sin \beta'_i]^T, \mathbf{k}_i = [\cos \gamma'_i \sin \gamma'_i]^T,$$

$$\mathbf{l}_i = [\cos \theta'_i \sin \theta'_i]^T, \mathbf{m}_i = [\cos(\phi + \psi_i) \sin(\phi + \psi_i)]^T \text{ and}$$

$$\beta'_i = \alpha_i + \beta_i, \gamma'_i = \alpha_i + \beta_i + \gamma_i + \phi, \theta'_i = \alpha_i + \beta_i + \gamma_i + \phi + \theta_i$$

The inverse kinematics solution for the manipulator can be derived from Eq. (1)

$$\begin{aligned} b_i &= (\mathbf{l}_i^T \mathbf{E} \mathbf{j}_i)^{-1} \mathbf{l}_i^T \mathbf{E} (\mathbf{T} - a_i \mathbf{i}_i - c_i \mathbf{k}_i - e_i \mathbf{m}_i) \\ d_i &= (\mathbf{j}_i^T \mathbf{E} \mathbf{l}_i)^{-1} \mathbf{j}_i^T \mathbf{E} (\mathbf{T} - a_i \mathbf{i}_i - c_i \mathbf{k}_i - e_i \mathbf{m}_i) \end{aligned} \quad (2)$$

where,  $\mathbf{E}$  is the right angle rotation matrix and defined as:  $\mathbf{E} = \begin{bmatrix} 0 & -1 \\ 1 & 0 \end{bmatrix}$

Geometric parameters for the U-shape and  $\Delta$ -shape fixed base 3-PRP manipulators are given in Tables 1 and 2. The CAD models are presented in Fig. 2.

**Table 1.** Geometric parameters for the U-shape fixed base 3PRP manipulator

Parameters	$\alpha_i$ (in degrees)	$\beta_i$ (in degrees)	$\gamma_i$ (in degrees)	$\theta_i$ (in degrees)
$i = 1$	180°	-90°	-90° + $\phi$	0°
$i = 2$	0°	+90°	+90° + $\phi$	0°
$i = 3$	90°	-90°	-90° + $\phi$	0°

**Table 2.** Geometric parameters for the  $\Delta$ -shape fixed base 3PRP manipulator

Parameters	$\alpha_i$ (in degrees)	$\beta_i$ (in degrees)	$\gamma_i$ (in degrees)	$\theta_i$ (in degrees)
$i = 1$	0°	120°	-90° + $\phi$	0°
$i = 2$	0°	60°	+90° + $\phi$	0°
$i = 3$	90°	-90°	-90° + $\phi$	0°

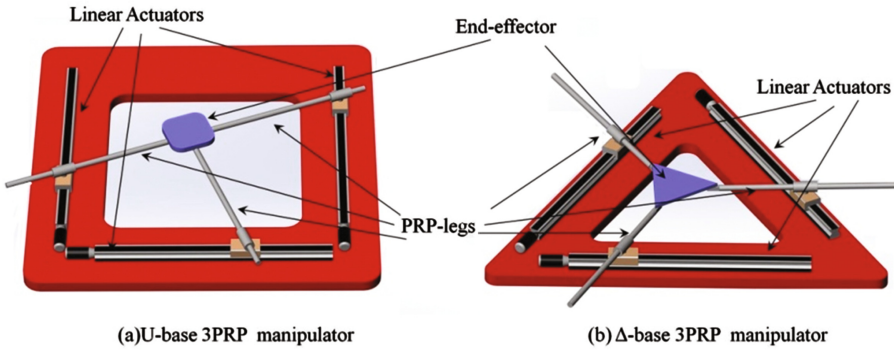


**Fig. 2.** CAD models of the U-shape and  $\Delta$ -shape fixed base 3-PRP manipulators

### 3 Jacobian and Singularities of the Manipulator

Velocity expression can be derived from the Eq. (1) by taking time derivative and eliminating the coefficient of  $\mathbf{l}_i$ , as below:

$$\mathbf{A} [\dot{\mathbf{T}} \quad \dot{\phi}]^T = \mathbf{B} \mathbf{b} \tag{3}$$

where,  $\mathbf{A}$  and  $\mathbf{B}$  are the forward and inverse Jacobian of the manipulators, respectively. These matrices are analytically given as follows:

$$\mathbf{A} = \begin{bmatrix} \mathbf{l}_1^T \mathbf{E}^T & -d_1 - c_1 \mathbf{l}_1^T \mathbf{k}_1 - e_1 \mathbf{l}_1^T \mathbf{m}_1 \\ \mathbf{l}_2^T \mathbf{E}^T & -d_2 - c_2 \mathbf{l}_2^T \mathbf{k}_2 - e_2 \mathbf{l}_2^T \mathbf{m}_2 \\ \mathbf{l}_3^T \mathbf{E}^T & -d_3 - c_1 \mathbf{l}_1^T \mathbf{k}_1 - e_1 \mathbf{l}_2^T \mathbf{m}_2 \end{bmatrix}, \mathbf{B} = \begin{bmatrix} \mathbf{l}_1^T \mathbf{E}^T \mathbf{j}_1 & 0 & 0 \\ 0 & \mathbf{l}_2^T \mathbf{E}^T \mathbf{j}_2 & 0 \\ 0 & 0 & \mathbf{l}_3^T \mathbf{E}^T \mathbf{j}_3 \end{bmatrix}$$

The kinematic Jacobain of the manipulator is given as:

$$\mathbf{J} = \mathbf{A}^{-1}\mathbf{B} \tag{4}$$

where, Matrix  $\mathbf{A}$  is never singular while matrix  $\mathbf{B}$  is singular only when the angle  $\phi = \pm 90^\circ$ , which is not possible for the manipulator within workspace, so neither serial nor parallel singularity is present in the manipulator. So this configuration is a singularity-free within its given workspace.

### 4 Error Modelling

In order to include the effect of joint clearances, the rotary joint the clearance is characterized by using a small distance  $\delta\rho_i$  between the points  $\mathbf{P}_i$  and  $\mathbf{P}'_i$  in the  $i^{th}$  link as shown in Fig. 3. To obtain the error for the end effector at point  $\mathbf{T}$  Eq. (1) is differentiated to obtain Eq. (5).

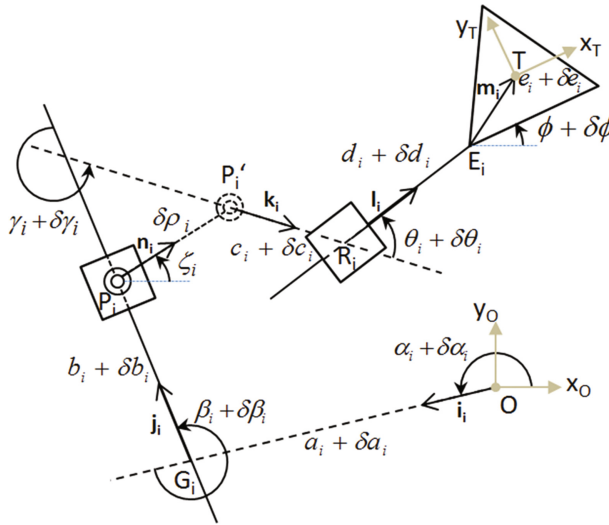


**Fig. 3.** Error variables in the joint parameters of 3PRP manipulator

$$\delta\mathbf{T} = \delta a_i \mathbf{i}_i + a_i \delta \alpha_i \mathbf{E} \mathbf{i}_i + \delta b_i \mathbf{j}_i + b_i \delta \beta'_i \mathbf{E} \mathbf{j}_i + \delta \rho_i \mathbf{n}_i + \delta c_i \mathbf{k}_i + c_i \delta \gamma'_i \mathbf{E} \mathbf{k}_i + \delta d_i \mathbf{l}_i + d_i \delta \theta'_i \mathbf{E} \mathbf{l}_i + e_i (\delta \phi + \delta \psi_i) \mathbf{E} \mathbf{m}_i, \quad i = 1, 2, 3 \tag{5}$$

$$\begin{aligned} \delta \beta'_i &= \delta \alpha_i + \delta \beta_i \\ \delta \gamma'_i &= \delta \alpha_i + \delta \beta_i + \delta \gamma_i + \delta \phi \\ \delta \theta'_i &= \delta \alpha_i + \delta \beta_i + \delta \gamma_i + \delta \phi + \delta \theta_i \end{aligned} \tag{6}$$

where,  $\delta\mathbf{T}$  and  $\delta\phi$  are the positioning and orientation error at the end effector.

Other variables namely,  $\delta a_i$ ,  $\delta \alpha_i$ ,  $\delta b_i$ ,  $\delta \beta_i$ ,  $\delta c_i$ ,  $\delta \gamma_i$ ,  $\delta d_i$ ,  $\delta \theta_i$ ,  $\delta e_i$  and  $\delta \psi_i$  show the variations in the geometric parameters of the link arrangement. Other than these effects, it is also introduced a joint distance which represents the joint clearance of a rotary joint and denoted as  $\delta \rho_i$ . The associated vector with this distance variable is  $\mathbf{n}_i = [\cos \zeta_i \quad \sin \zeta_i]^T$ , by substituting the values of Eq. (6) in Eq. (5) and eliminating the variable  $\delta d_i$ , it gives

$$\begin{aligned} \mathbf{l}_i^T \mathbf{E}^T \delta \mathbf{T} &= \delta a_i \mathbf{l}_i^T \mathbf{E}^T \mathbf{i}_i + \delta \alpha_i [\mathbf{l}_i^T (a_i \mathbf{i}_i + b_i \mathbf{j}_i + c_i \mathbf{k}_i) + d_i] + \delta b_i \mathbf{l}_i^T \mathbf{E}^T \mathbf{j}_i \\ &+ \delta \beta_i [\mathbf{l}_i^T (b_i \mathbf{j}_i + c_i \mathbf{k}_i) + d_i] + \delta \rho_i \mathbf{l}_i^T \mathbf{E}^T \mathbf{n}_i + \delta c_i \mathbf{l}_i^T \mathbf{E}^T \mathbf{k}_i + \delta \gamma_i (c_i \mathbf{l}_i^T \mathbf{k}_i + d_i) \\ &+ d_i \delta \theta_i + \delta \phi (c_i \mathbf{l}_i^T \mathbf{k}_i + d_i + e_i \mathbf{l}_i^T \mathbf{m}_i) + \delta e_i \mathbf{l}_i^T \mathbf{E}^T \mathbf{m}_i + \delta \psi_i e_i \mathbf{l}_i^T \mathbf{m}_i \end{aligned} \quad (7)$$

If substituting the values of  $i = 1, 2, 3$  in Eq. (7) and arrange it in vector form as:

$$\begin{aligned} \mathbf{A} \begin{bmatrix} \delta x \\ \delta y \\ \delta \phi \end{bmatrix} &= \mathbf{H}_a \begin{bmatrix} \delta a_1 \\ \delta a_2 \\ \delta a_3 \end{bmatrix} + \mathbf{H}_\alpha \begin{bmatrix} \delta \alpha_1 \\ \delta \alpha_2 \\ \delta \alpha_3 \end{bmatrix} + \mathbf{B} \begin{bmatrix} \delta b_1 \\ \delta b_2 \\ \delta b_3 \end{bmatrix} + \mathbf{H}_\beta \begin{bmatrix} \delta \beta_1 \\ \delta \beta_2 \\ \delta \beta_3 \end{bmatrix} + \mathbf{H}_\rho \begin{bmatrix} \delta \rho_1 \\ \delta \rho_2 \\ \delta \rho_3 \end{bmatrix} \\ &+ \mathbf{H}_c \begin{bmatrix} \delta c_1 \\ \delta c_2 \\ \delta c_3 \end{bmatrix} + \mathbf{H}_\gamma \begin{bmatrix} \delta \gamma_1 \\ \delta \gamma_2 \\ \delta \gamma_3 \end{bmatrix} + \mathbf{H}_\theta \begin{bmatrix} \delta \theta_1 \\ \delta \theta_2 \\ \delta \theta_3 \end{bmatrix} + \mathbf{H}_e \begin{bmatrix} \delta e_1 \\ \delta e_2 \\ \delta e_3 \end{bmatrix} + \mathbf{H}_\psi \begin{bmatrix} \delta \psi_1 \\ \delta \psi_2 \\ \delta \psi_3 \end{bmatrix} \end{aligned} \quad (8)$$

By multiplying  $\mathbf{A}^{-1}$  on both sides, using Eq. (4) and replacing  $\mathbf{J}_q$  with  $\mathbf{A}^{-1} \mathbf{H}_q$ , where  $q \in \{a, \alpha, \beta, \rho, c, \gamma, d, \theta, e, \psi\}$ . The error sensitivity equation for the manipulator is given as:

$$\begin{aligned} \begin{bmatrix} \delta x \\ \delta y \\ \delta \phi \end{bmatrix} &= \mathbf{J}_a \begin{bmatrix} \delta a_1 \\ \delta a_2 \\ \delta a_3 \end{bmatrix} + \mathbf{J}_\alpha \begin{bmatrix} \delta \alpha_1 \\ \delta \alpha_2 \\ \delta \alpha_3 \end{bmatrix} + \mathbf{J}_b \begin{bmatrix} \delta b_1 \\ \delta b_2 \\ \delta b_3 \end{bmatrix} + \mathbf{J}_\beta \begin{bmatrix} \delta \beta_1 \\ \delta \beta_2 \\ \delta \beta_3 \end{bmatrix} + \mathbf{J}_\rho \begin{bmatrix} \delta \rho_1 \\ \delta \rho_2 \\ \delta \rho_3 \end{bmatrix} \\ &+ \mathbf{J}_c \begin{bmatrix} \delta c_1 \\ \delta c_2 \\ \delta c_3 \end{bmatrix} + \mathbf{J}_\gamma \begin{bmatrix} \delta \gamma_1 \\ \delta \gamma_2 \\ \delta \gamma_3 \end{bmatrix} + \mathbf{J}_\theta \begin{bmatrix} \delta \theta_1 \\ \delta \theta_2 \\ \delta \theta_3 \end{bmatrix} + \mathbf{J}_e \begin{bmatrix} \delta e_1 \\ \delta e_2 \\ \delta e_3 \end{bmatrix} + \mathbf{J}_\psi \begin{bmatrix} \delta \psi_1 \\ \delta \psi_2 \\ \delta \psi_3 \end{bmatrix} \end{aligned} \quad (9)$$

The coefficients of the error vectors in the above relation are the corresponding sensitivity matrices related to each error variables. These analytical expressions are validated using the virtual prototype with the help of MSC ADAMS software. Further, these relations are used for accuracy and sensitivity analyses in the following section.

## 5 Error Sensitivity Analysis

Errors due to joint (bearing) clearances and the actuator inaccuracies (least count errors) may cause alteration in the end-effector's pose which cannot be compensated. Other structural parameter errors related to the link lengths and actuator indexing errors can

be compensated by the help of the calibration techniques or parameter identification methods suggested for parallel manipulators. But the error caused due to the presence of clearances, actuator inaccuracies and encoder least count errors are non-compensable by such calibration techniques. Therefore, pose errors are estimated due to the joint clearances, actuator inaccuracies and encoder least count errors using commercially available data for rotary and prismatic joints and, encoder resolution. For the rotary joint, joint clearances are assumed as:

$0 \text{ mm} \leq \delta\rho_i \leq 0.016 \text{ mm}$  and the contact angle  $\zeta_i$  can vary from 0 to  $2\pi$  radians, where  $\delta\rho_i$  is the center to center distance of the mating bodies of the rotary joints. The error variable  $\delta\theta_i$  depends on the joint clearance of the prismatic joint and angular deviation because of that which is  $-0.04^\circ \leq \delta\theta_i \leq 0.04^\circ$  and the least count error is taken as half of the least count which cannot be detected by the encoders here taken as  $0 \text{ mm} \leq \delta b_i \leq 0.025 \text{ mm}$ . The analytical error prediction model is solved simultaneously as an optimization problem using the genetic algorithms. For numerical computation, the Matlab function namely, “*ga*” an in-built genetic algorithms optimization solver is used. The test region for the error sensitivity analysis is considered as a square area of  $80 \text{ mm} \times 80 \text{ mm}$  for the given actuator span of  $200 \text{ mm}$  in all three legs. To compare the effect of the non-compensable errors in U-shape and  $\Delta$ -shape fixed base parallel configurations the data for joint clearances and encoder resolutions are taken from the industrial product catalogues [7]. Local maximum possible pose errors of the end-effector are obtained through the optimization code for the given workspace region for the constant end-effector orientation. Error contour plots are presented in Figs. 4 and 5.

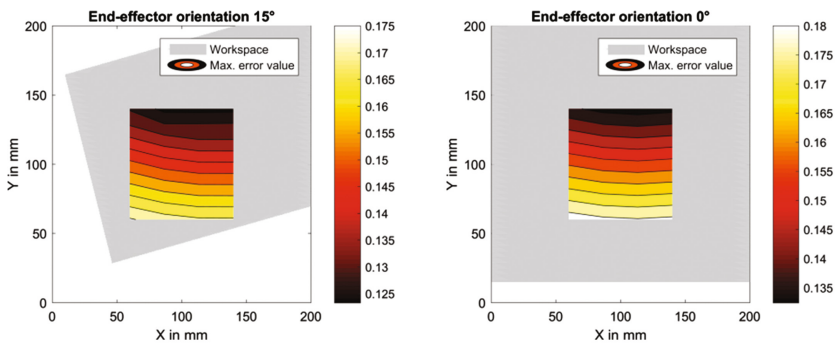


**Fig. 4.** Non-compensable error contour plots of the U-shape fixed base 3-PRP PPM

The local maximum position errors due to the non-compensable errors in U-shape and  $\Delta$ -shape fixed base parallel configurations are presented in Figs. 4 and 5, respectively. The result shows that the pose errors due the non-compensable errors for the selected workspace region are varying from  $110 \mu\text{m}$  to  $150 \mu\text{m}$  for U-shape 3-PRP PPM and  $70 \mu\text{m}$  to  $95 \mu\text{m}$  for  $\Delta$ -shape 3-PRP PPM. From the results, it is observed that  $\Delta$ -shape (symmetric shape) fixed base configuration performs better than U-shape fixed base configurations in presence of non-compensable errors for 3-PRP kinematic arrangement.

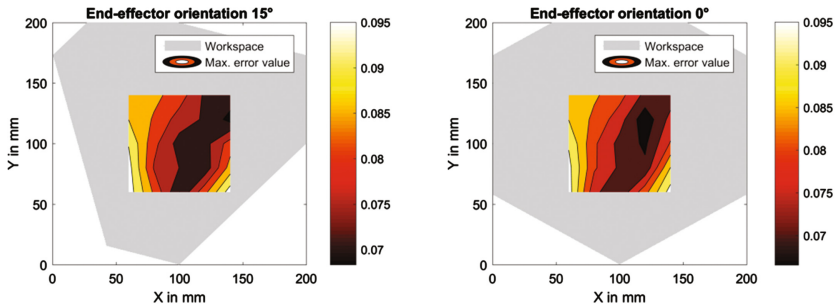


Fig. 5. Non-compensable error contour plots of the  $\Delta$ -shape fixed base 3-PRP PPM

## 6 Conclusions

In this paper, an analytical error prediction model for the planar 3-PRP parallel configuration is derived by considering all possible mechanical inaccuracies. Solution for the joint parameter's dependency on the orientation angle of the end-effector is solved and demonstrated. From the results, it is found that the  $\Delta$ -shape fixed base configuration is less sensitive to the non-compensable errors. These non-compensable errors cannot be compensated by the offline calibration method. But, it can be minimized or compensated by using a task-space motion control strategy in trajectory tracking, which would be considered as a future work.

**Acknowledgments.** This research was supported and funded in part by the Council of Scientific & Industrial Research (CSIR) India, (22(0698)/15/EMR-II/5767).

## References

1. Chablat, D., Staicu, S.: Kinematics of A 3-PRP planar parallel robot. *UPB Sci. Bull. Ser. D Mech. Eng.* **71**, 3–16 (2009)
2. Huang, Z., Li, Q., Ding, H.: *Theory of Parallel Mechanisms*. Springer, Dordrecht (2012)
3. Joubair, A., Slamani, M., Bonev, I.A.: A novel XY-Theta precision table and a geometric procedure for its kinematic calibration. *Robot. Comput. Integr. Manuf.* **28**, 57–65 (2012)
4. Liu, Y., Wu, J., Wang, L., Wang, J.: Parameter identification algorithm of kinematic calibration in parallel manipulators. *Adv. Mech. Eng.* **8**, 1–16 (2016)
5. Singh, Y.: Performance investigations on mechanical design and motion control of planar parallel manipulators, Ph.D. thesis, Indian Institute of Technology Indore (2016)
6. Wijk, V.V., Herder, J.L.: Guidelines for low mass and low inertia dynamic balancing of mechanisms and robotics. In: *Advances in Robotics Research*, pp. 21–30. Springer (2009)
7. Wu, G., Bai, S., Kepler, J.A., Caro, S.: Error modeling and experimental validation of a planar 3-PPR parallel manipulator with joint clearances. *J. Mech. Robot.* **4**, 041008-1–041008-12 (2012)
8. Yu, A., Bonev, I.A., Zsombor-Murray, P.: Geometric approach to the accuracy analysis of a class of 3-DOF planar parallel robot. *Mech. Mach. Theor.* **43**, 364–375 (2008)